

MICROCOPY RESOLUTION TEST CHART  
NATIONAL BUREAU OF STANDARDS-1963-A

AT E 301684

2

**AD-A154 376**

**DNA-TR-84-307**

**NITROGEN CHEMISTRY IN SEA LEVEL AIR FOLLOWING  
LARGE RADIATION DOSES**

**Murray Scheibe  
Mission Research Corp  
P.O. Drawer 719  
Santa Barbara, CA 93102-0719**

**15 June 1984**

**Technical Report**

**CONTRACT No. DNA 001-80-C-0151**

**APPROVED FOR PUBLIC RELEASE;  
DISTRIBUTION UNLIMITED.**

**THIS WORK WAS SPONSORED BY THE DEFENSE NUCLEAR AGENCY  
UNDER RDT&E RMSS CODE B322081466 S99QAXHD00004 H2590D.**

**DTIC FILE COPY**

**Prepared for  
Director  
DEFENSE NUCLEAR AGENCY  
Washington, DC 20305-1000**

**DTIC  
ELECTE  
S JUN 3 1985 D  
B**

**85 03 29 016**

Destroy this report when it is no longer needed. Do not return to sender.

PLEASE NOTIFY THE DEFENSE NUCLEAR AGENCY,  
ATTN: STTI, WASHINGTON, DC 20305-1000, IF YOUR  
ADDRESS IS INCORRECT, IF YOU WISH IT DELETED  
FROM THE DISTRIBUTION LIST, OR IF THE ADDRESSEE  
IS NO LONGER EMPLOYED BY YOUR ORGANIZATION.



UNCLASSIFIED

SECURITY CLASSIFICATION OF THIS PAGE

## REPORT DOCUMENTATION PAGE

1a. REPORT SECURITY CLASSIFICATION <b>UNCLASSIFIED</b>		1b. RESTRICTIVE MARKINGS	
2a. SECURITY CLASSIFICATION AUTHORITY		3. DISTRIBUTION / AVAILABILITY OF REPORT Approved for public release; distribution is unlimited.	
2b. DECLASSIFICATION / DOWNGRADING SCHEDULE		5. MONITORING ORGANIZATION REPORT NUMBER(S) <b>DNA-TR-84-307</b>	
4. PERFORMING ORGANIZATION REPORT NUMBER(S) <b>MRC-R-845</b>		7a. NAME OF MONITORING ORGANIZATION Director Defense Nuclear Agency	
6a. NAME OF PERFORMING ORGANIZATION <b>Mission Research Corporation</b>	6b. OFFICE SYMBOL (if applicable)	7b. ADDRESS (City, State, and ZIP Code) <b>Washington, DC 20305-1000</b>	
6c. ADDRESS (City, State, and ZIP Code) <b>P. O. Drawer 719 Santa Barbara, CA 93102-0719</b>		9. PROCUREMENT INSTRUMENT IDENTIFICATION NUMBER <b>DNA 001-80-C-0151</b>	
8a. NAME OF FUNDING / SPONSORING ORGANIZATION	8b. OFFICE SYMBOL (if applicable)	10. SOURCE OF FUNDING NUMBERS	
8c. ADDRESS (City, State, and ZIP Code)		PROGRAM ELEMENT NO <b>62715H</b>	PROJECT NO <b>S99QAXH</b>
		TASK NO <b>D</b>	WORK UNIT ACCESSION NO <b>DH005185</b>
11. TITLE (Include Security Classification) <b>NITROGEN CHEMISTRY IN SEA LEVEL AIR FOLLOWING LARGE RADIATION DOSES</b>			
12. PERSONAL AUTHOR(S) <b>Murray Scheibe</b>			
13a. TYPE OF REPORT <b>Technical</b>	13b. TIME COVERED FROM <b>80Feb01</b> TO <b>81Sep30</b>	14. DATE OF REPORT (Year, Month, Day) <b>1984 June 15</b>	15. PAGE COUNT <b>40</b>
16. SUPPLEMENTARY NOTATION This work was sponsored by the Defense Nuclear Agency under RDT&E RMSS Code B322081466 S99QAXHD00004 H2590D.			
17. COSATI CODES		18. SUBJECT TERMS (Continue on reverse if necessary and identify by block number)	
FIELD	GROUP	Nuclear Burst      Radiation Chemistry	
<b>4</b>	<b>1</b>	Nitric Acid      Bomblight	
<b>6</b>	<b>18</b>	Nitrous Oxide	
19. ABSTRACT (Continue on reverse if necessary and identify by block number)			
<p>The electron densities near a large yield nuclear burst during the first few seconds can impact the performance of terminal defense radars. The main chemical parameters which determine the electron density in this situation are the electron attachment and detachment rates. This report describes work done to determine the production of <math>\text{HNO}_3</math> and <math>\text{N}_2\text{O}</math>, good attachers of electrons, by the burst radiation and the effect on electron detachment caused by bomblight induced photochemical reactions.</p> <p>In the matter of the production of <math>\text{HNO}_3</math> and <math>\text{N}_2\text{O}</math> the results of an experiment done at Oak Ridge were used to revise the reaction scheme used in the chemical integration code used to simulate the nuclear case. It was found that the irradiation time is a critical factor in the production of <math>\text{HNO}_3</math>. An order of magnitude or more less <math>\text{HNO}_3</math> was produced</p>			
20. DISTRIBUTION / AVAILABILITY OF ABSTRACT <input type="checkbox"/> UNCLASSIFIED/UNLIMITED <input checked="" type="checkbox"/> SAME AS RPT <input type="checkbox"/> DTIC USERS		21. ABSTRACT SECURITY CLASSIFICATION <b>UNCLASSIFIED</b>	
22a. NAME OF RESPONSIBLE INDIVIDUAL <b>Betty L. Fox</b>		22b. TELEPHONE (Include Area Code) <b>(202) 325-7042</b>	22c. OFFICE SYMBOL <b>DNA/STTI</b>

UNCLASSIFIED

SECURITY CLASSIFICATION OF THIS PAGE

19. ABSTRACT (continued)

in the nuclear cases simulated than in the laboratory experiment where the irradiation times were longer.  $\text{HNO}_3$ , however might still be an important attachment of electrons in the nuclear case.

The bombhight does not appear to affect very strongly the electron densities in the air outside the fireball. The delayed gamma-ray radiation tends to overwhelm the bombhight effect.

UNCLASSIFIED

SECURITY CLASSIFICATION OF THIS PAGE

## TABLE OF CONTENTS

<u>Section</u>		<u>Page</u>
1	INTRODUCTION	1
2	RADIATION INDUCED NITROGEN AND HYDROGEN CHEMISTRY	3
3	OAK RIDGE EXPERIMENT	8
4	ION-ION RECOMBINATION	10
5	NO <sub>2</sub> NEUTRAL CLUSTERS	12
6	CALCULATIONAL SIMULATION OF EXPERIMENT	14
7	NUCLEAR EFFECTS CALCULATIONS	18
8	BOMBLIGHT EFFECTS	22
9	CONCLUSIONS	26
	REFERENCES	27



Accession For	
NTIS GRA&I	<input checked="" type="checkbox"/>
DTIC TAB	<input type="checkbox"/>
Unannounced	<input type="checkbox"/>
Justification _____	
By _____	
Distribution/ _____	
Availability Codes	
Dist	Avail and/or Special
A-1	

## SECTION 1 INTRODUCTION

The electron densities near a large yield nuclear burst (i.e., within about one fireball radius) during the first few seconds can impact the performance of terminal defense radars. The main chemical parameters which determine the electron density in this situation are the electron attachment and detachment rates.

The photochemical process caused by bomb light are poorly understood and we thought that these mechanisms might increase the electron density at the time of thermal maximum sufficiently to degrade these radars. Increased attachment on the other hand would decrease the electron density and could be caused by species which are produced by the high energy radiation emanating from the nuclear weapon (X-rays, neutrons, gamma rays). The production of long lived species, such as NO, NO<sub>2</sub>, HNO<sub>2</sub>, HNO<sub>3</sub> and N<sub>2</sub>O is not, as yet, well understood. In particular HNO<sub>3</sub> and, under certain conditions, N<sub>2</sub>O are known to be efficient attachers of electrons.

In the work covered in this report we have attempted to determine the production of HNO<sub>3</sub> and N<sub>2</sub>O in the nuclear case. In this work we used the results from an Oak Ridge experiment to be described to improve the chemistry scheme in our computer code.

The first section which follows will describe the nitrogen and hydrogen chemistry governing the production of HNO<sub>3</sub> and N<sub>2</sub>O. The next section describes the Oak Ridge experiment and its results. The following



two sections describe the revisions made to our chemistry code to increase agreement between the code and the experiment. The next section shows the results predicted by our code when simulating the experiment and the degree of agreement and the following section describes the results of the revised code in simulation of a nuclear burst. The next to the last section describes our efforts to calculate the effects of photodetachment and photodissociation on the electron densities near a burst. The result of this was negative. The final section contains our conclusions.

## SECTION 2

### RADIATION INDUCED NITROGEN AND HYDROGEN CHEMISTRY

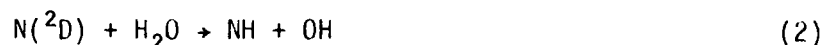
The production of long lived nitrogen minor species is initiated by the deposition in the surrounding air of the high energy radiation from the nuclear weapon. The degradation of this energy is accompanied by the production, in addition to electron and ions, of species not normally found in ambient air in appreciable quantities. Table 1 contains a list of these species and the yields per ion pair. Also listed is the ion distribution. These numbers represent the best estimate<sup>1,2</sup> but have considerable uncertainties associated with them.

**Table 1. Species production per ion-pair.**

$N_2^+$	0.63
$O_2^+$	0.16
$N^+$	0.14
$O^+$	0.07
$N_2(A)$	0.60
$O_2(^1\Delta)$	0.30
$O_2(^1\Sigma)$	0.10
$O(^3P)$	0.21
$O(^1D)$	0.12
$N(^4S)$	0.60
$N(^2D)$	0.64

The species ( $O_2(^1\Delta)$ ,  $O_2(^1\Sigma)$ ,  $O(^1D)$ ,  $N_2(A)$  and  $N(^2D)$ ) are metastable excited electronic states.  $O(^3P)$  and  $N(^4S)$  are the oxygen and nitrogen atom ground electronic states.

The production of species such as  $NO$ ,  $NO_2$ ,  $HNO_2$ , and  $HNO_3$  is highly dependent on the production and subsequent chemistry of  $N(^4S)$  and  $N(^2D)$ . Virtually all of the  $N(^2D)$  enters into the two following reactions.



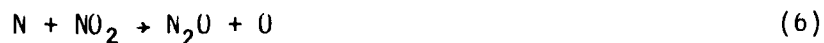
(When an excited state is not indicated the ground state is assumed.) At altitudes above sea level reaction 1 is by far the dominant mechanism depleting the  $N(^2D)$ . At sea level altitudes, however, the water vapor density is large enough to make reaction 2 account for as much as half of the  $N(^2D)$  depletion. The products of reaction 2 are uncertain but are probably as shown.<sup>3</sup> The introduction of  $NH$  adds even more uncertainty into the chemistry since very little is known about the reactions of this species. The rate coefficient of only the reaction



has been measured<sup>4</sup> but the products are unknown. We had to estimate or guess the other reactions and rate coefficients involving  $NH$ .

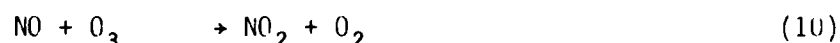
The ground state nitrogen,  $N(^4S)$ , will primarily enter into the following reactions.





Reactions 4 through 8 are those mainly responsible for the conversion of the initially formed atomic nitrogen back to  $\text{N}_2$  or to  $\text{NO}$  and  $\text{N}_2\text{O}$ .

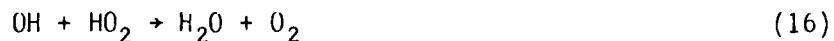
The sum of the  $\text{N}(^4\text{S})$  and  $\text{N}(^2\text{D})$  formed initially is (from Table 1) 1.24 per ion-pair. To this must be added the  $\text{N}^+$  (0.14 per ion-pair) which will react with air species to yield  $\text{N}(^4\text{S})$ ,  $\text{N}(^2\text{D})$ ,  $\text{NO}$ ,  $\text{NO}_2$  or  $\text{N}_2\text{O}$ . This 1.38 "odd nitrogen" per ion-pair is the pool from which  $\text{N}_2\text{O}$  and  $\text{NO}_x$ , where  $x = 1$  or  $2$ , will eventually be formed. The  $\text{N}_2\text{O}$  is extremely stable with regard to reactions with other neutral species. Some of the  $\text{NO}_x$  will continue to react according to the following major reactions



The above reactions will cause some of the  $\text{NO}_x$  to be converted to  $\text{HNO}_y$ , where  $y = 2$  or  $3$ .

Many of the reactions listed heretofore involve H, OH and HO<sub>2</sub> as reactants. Some of the "odd hydrogen" comes from reaction 2 and other neutral reactions. The bulk of the odd hydrogen, however, is generated by chemical evolution of the positive ions. Unless the electron density is extremely high (greater than about 10<sup>15</sup> cm<sup>-3</sup>) virtually all the initial ions undergo a complex evolution prior to recombination which yields ions of the form H<sub>3</sub>O<sup>+</sup> · (H<sub>2</sub>O)<sub>n</sub>, where n can be zero through four in our code and higher than four in the real world. Obviously at some point in this ion hydration scheme an H<sub>2</sub>O is broken up and an OH radical released. When the H<sub>3</sub>O<sup>+</sup> · (H<sub>2</sub>O)<sub>n</sub> recombines, either with an electron or with a negative ion, an H is released. This will generally combine with O<sub>2</sub> to form HO<sub>2</sub>. Thus more than two odd hydrogen species are formed per ion pair (the odd hydrogen formed by reaction 2 must be added to those formed by the ion hydration and recombination).

These species, however, are not long-lived. Several processes act to reconstitute water vapor or H<sub>2</sub>. The most important of these is the reaction



This has a rather large rate coefficient at sea level densities (~ 10<sup>-10</sup> cm<sup>3</sup>/sec) and the size of this rate coefficient controls the amount of odd hydrogen present and causes it to decay rapidly when the ionizing source is turned off.

The amount and distribution of odd nitrogen species will greatly depend on the chemical scheme, the main features of which have been described above. The size of the radiation dose and its duration will also have an impact. If the dose is large enough, the air will be heated considerably.

Because of the size of reaction 16, the amount of the  $\text{HNO}_2$  and  $\text{HNO}_3$  formed by the above reaction scheme is minimal. For the radiation pulses characteristic of nuclear bursts, i.e., large doses of about a millisecond or less duration, we obtain at most 0.1 combined  $\text{HNO}_2$  and  $\text{HNO}_3$  produced per ion pair. In general, the shorter the pulse the less we obtain.

### SECTION 3 OAK RIDGE EXPERIMENT

Oak Ridge National Laboratory conducted an experiment<sup>5</sup> in which a parcel of air was irradiated with a beam of 1.0 MeV electrons and the gas was periodically analyzed by infrared spectrophotometry. The dose rate was  $1.73 \times 10^{20}$  eV/min for an air volume of  $3.80 \times 10^2$  cm<sup>3</sup>. This corresponds to an ionization rate of  $2.2 \times 10^{14}$  ion-pairs/cm<sup>3</sup>-sec. This is less, by many orders of magnitude, than that experienced by a parcel of air close to but outside the nuclear fireball. The sample was, however, irradiated for up to 60 minutes or more and this is many orders of magnitude longer than the neutron and X-ray pulse from a nuclear weapon. The total integrated dose is of the order, or greater, than what might be expected in the nuclear case. The experiment showed that for a total dose of about  $8 \times 10^{16}$  ion-pairs/cm<sup>3</sup>, there were  $8 \times 10^{16}$  cm<sup>-3</sup> of HNO<sub>3</sub> formed and  $2.7 \times 10^{16}$  cm<sup>-3</sup> of N<sub>2</sub>O formed. The production of HNO<sub>3</sub> continued beyond that dose at a rate linear to the dose until all the water vapor was depleted. Beyond that point the HNO<sub>3</sub> disappeared rapidly and NO<sub>2</sub> was formed at the same rate as that of the HNO<sub>3</sub> depletion. When all the HNO<sub>3</sub> was gone the rate of NO<sub>2</sub> production per ion-pair slowed considerably. N<sub>2</sub>O continued to be produced throughout the whole dose range but decreased somewhat at high integrated doses. No mention was made of HNO<sub>2</sub> and we assumed that none was observed. In a variation of the experiment NO<sub>2</sub> was initially added to the air sample. In that case no HNO<sub>3</sub> was produced and only about half the N<sub>2</sub>O.

The nuclear cases of interest correspond to total doses which would not deplete all the H<sub>2</sub>O. At doses such that the H<sub>2</sub>O would be significantly depleted, the air temperature would become high enough to

thermally dissociate the  $N_2O$  and  $HNO_3$  and cause the chemistry scheme to be different. In the experiment the irradiation was spread over a time long enough that cooling by the walls probably kept the air sample from getting significantly hotter than ambient.

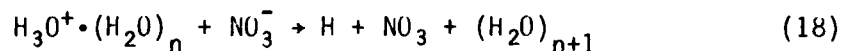
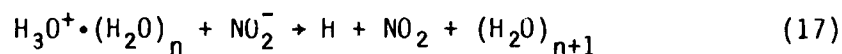
Our multispecies chemical integration code using the neutral chemistry scheme described earlier predicted a much lower production rate for  $HNO_3$  than was observed in this experiment. Since  $HNO_3$  is a very efficient attacher of electrons, and since the value we calculate is far too low, we reviewed our chemistry looking for changes that would increase the  $HNO_3$  production and bring it into agreement with the experiment. These revisions could impact the nuclear case significantly.



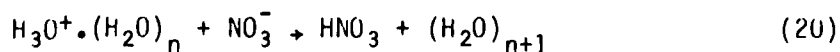
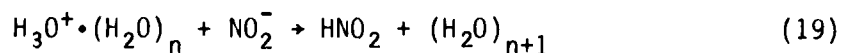
## SECTION 4 ION-ION RECOMBINATION

It was noted earlier that the positive ions produced initially by the weapon radiation are transformed into ions of the type  $H_3O^+ \cdot (H_2O)_n$ . At sea level densities the electron attachment coefficient is very large (about  $10^8 \text{ sec}^{-1}$ ) and unless the electron density is very high the electrons will attach before they recombine. The primary negative ion initially formed,  $O_2^-$ , will be involved in a complex chemical scheme in which it is transformed to  $NO_2^-$  and  $NO_3^-$ . Ions such as  $O_3^-$ ,  $O_4^-$ ,  $CO_3^-$ ,  $CO_4^-$  and  $OH^-$  act as intermediates in this transformation. The  $NO_2^-$  and  $NO_3^-$  may also be hydrated, i.e., have one or more attached water molecules.

The products of the recombination of  $H_3O^+ \cdot (H_2O)_n$  and  $NO_2^-$  and  $NO_3^-$  are unknown and we have heretofore assumed the following



The choice was arbitrary and could have been



In fact, from an energetic point of view, reactions 19 and 20 would be preferred. Under conditions which would allow all the ions to convert to those shown in the right-hand side of the above reactions, i.e., when the dose rate and electron density are small, we would expect a yield of about one  $\text{HNO}_2$  or  $\text{HNO}_3$  per ion pair just from reactions 19 and 20. This would certainly contribute greatly in the Oak Ridge experiment. In the nuclear case the dose rates and electron densities are much higher and the yield of  $\text{HNO}_2$  and  $\text{HNO}_3$  would be somewhat less.

In addition, when reactions 17 and 18 are used the free hydrogen released combines with  $\text{O}_2$  to form  $\text{HO}_2$  which then can react with  $\text{OH}$  by reaction 16. When reactions 19 and 20 are used instead of 17 and 18 the hydrogen atom is tied up in  $\text{HNO}_2$  and  $\text{HNO}_3$ . These species can also react with  $\text{OH}$  to yield  $\text{H}_2\text{O}$  but with much smaller rates than with  $\text{HO}_2$ . This means the water vapor reformation will be slowed and the  $\text{OH}$  will be around longer. This should enhance the  $\text{HNO}_2$  and  $\text{HNO}_3$  production by reactions 14 and 15.

## SECTION 5 NO<sub>2</sub> NEUTRAL CLUSTERS

Another change that was made in our chemistry scheme was that the species N<sub>2</sub>O<sub>5</sub> and HO<sub>2</sub>NO<sub>2</sub> were added. These species are formed in the following reactions



These species have been observed and measured rate coefficients for reactions 21 and 22 have been reported.<sup>6,7</sup> At temperatures above about 300 K the species N<sub>2</sub>O<sub>5</sub> did not have much importance and we will therefore not discuss reaction 21 any further. The species HO<sub>2</sub>NO<sub>2</sub> did have a significant effect. The only reported reactions involving this species are



Reaction 24 has an activation energy of about 0.3 eV and is therefore not very important at ambient temperatures. In the nuclear case, however, it may be important under high dose conditions. We have assumed two channels for reaction 23 and divided the reported rate coefficient equally between them. The first channel yields HO<sub>2</sub> and HNO<sub>3</sub> as the products. The second yields H<sub>2</sub>O + O<sub>2</sub> and NO<sub>2</sub> as the products. In the first case the rate coefficient is less than for the direct formation of HNO<sub>3</sub> from OH and NO<sub>2</sub>

(reaction 15). In the second case the rate coefficient is much less than the direct reaction of OH and HO<sub>2</sub> (reaction 16). Thus having a substantial amount of the NO<sub>2</sub> and HO<sub>2</sub> tied up as HO<sub>2</sub>NO<sub>2</sub> would decrease the rate formation of HNO<sub>3</sub> and the rate of reformation of water vapor. Reducing the rate of water reformation would, however, extend the longevity of OH and this would enhance the formation of both HNO<sub>2</sub> and HNO<sub>3</sub> by reactions 14 and 15. As it turns out the longer persistence of OH seems to dominate in the Oak Ridge experiment but in the nuclear case the net effect is minimal for a variety of reasons.

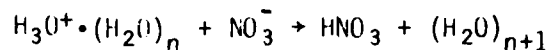
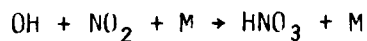
## SECTION 6 CALCULATIONAL SIMULATION OF EXPERIMENT

We have run our multi-species chemical integration code to simulate the Oak Ridge experiment. Our code integrates the coupled rate equations for electrons, 27 neutral species, 27 positive ion species, and eleven negative ion species. The code contains over 450 reactions in addition to the two-body and three-body ion-ion recombination reactions. Many of the latter reactions are lumped together in our code. This is possible because we assume the same rate coefficient for all two-body recombination and similarly for all three-body recombination.

A constant ionization rate of  $2.2 \times 10^{14}$  ion-pairs/cm<sup>3</sup>-sec was applied to air which contained about 0.1 percent H<sub>2</sub>O by volume. The reaction scheme included reactions 25 and 26 rather than reactions 23 and 24 and also included HO<sub>2</sub>NO<sub>2</sub> and N<sub>2</sub>O<sub>5</sub>. The code was run out to almost 5000 seconds which corresponded to a total dose rate of about  $10^{18}$  ion-pairs/cm<sup>3</sup>. The initial temperature was 298 K but the air was allowed to heat about 0.5 K per second to a maximum of 360K. It reached this maximum at a total dose of about  $2.5 \times 10^{16}$  ion-pairs/cm<sup>3</sup> or at about 120 seconds.

Our calculational results are in fair agreement with the experiment. Our HNO<sub>3</sub> production is about 0.6 per ion-pair and the HNO<sub>2</sub> production is 0.1 per ion-pair. This compares with a value of 1.0 for HNO<sub>3</sub> in the experiment and zero HNO<sub>2</sub>. The N<sub>2</sub>O production is in even better agreement. We obtained a value of 0.3 N<sub>2</sub>O per ion-pair. The experimental value was 0.34.

About 80 to 90 percent of the  $\text{HNO}_3$  is made, as expected, by reactions 15 and 20, i.e.,

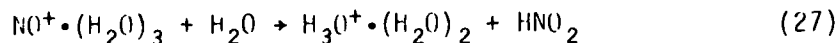


The remainder is made by other reactions, including reaction 23. A significant amount of  $\text{HNO}_3$  is destroyed by the reactions



Both of these are reactions for which the rate coefficients have been measured and it is reaction 26 which makes  $\text{HNO}_3$  potentially important in the nuclear case.

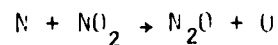
The main production of  $\text{HNO}_2$ , surprisingly, is neither reaction 14 nor 19 but reaction 25. The reaction



also contributes. The main destruction mechanism of  $\text{HNO}_2$  is



The main production of  $\text{N}_2\text{O}$  is through reaction 6, i.e.,



As the total dose increases beyond about  $2 \times 10^{16}$ , the increased temperature makes its effect felt. The  $\text{HO}_2\text{NO}_2$  concentration drops significantly as does the OH and  $\text{HO}_2$  concentrations. The  $\text{HO}_2\text{NO}_2$  is very weakly bound and an increase in temperature of just 50 K causes the large drop in its concentration. The OH can react more rapidly with the free  $\text{HO}_2$  and disappears more quickly. This reduces the production of  $\text{HNO}_3$  and causes the  $\text{HNO}_3$  concentration to drop dramatically to insignificance. (This suggests that the experiment did not involve any temperature increase.)

The  $\text{HNO}_2$  and  $\text{N}_2\text{O}$  production per ion-pair, however, remain about the same as before at these large doses. Before the temperature increases, the calculated  $\text{HNO}_3$  production is about 60 percent of what was obtained in the experiment. We consider this fair agreement but more  $\text{HNO}_3$  production is needed in the calculation to get better agreement. There are a number of possible ways this may occur. One way is if the amount of ground state and excited nitrogen atoms produced during the initial energy deposition is more than we have assumed. The values given in Table 1 are the result of calculations using both theoretical and measured cross sections and a number of uncertainties are involved. It is quite possible more odd nitrogen is formed than is shown in Table 1.

Another possibility is that the rate coefficient we have used for reaction 16, i.e.,



is too large. This is a measured value but it seems to be pressure dependent and this is not yet understood. The uncertainty in this rate is as much as a factor of two.<sup>6,7</sup>

Still another possibility to increase the  $\text{HNO}_3$  production is that there are reactions which convert  $\text{HNO}_2$  to  $\text{HNO}_3$ . Some possible reactions which accomplish this are





## SECTION 7

### NUCLEAR EFFECTS CALCULATIONS

Both a set of sequential bursts and a single burst (larger than any of the sequential bursts) were calculated to simulate the effect on the atmosphere of the prompt ionizing radiation from a nuclear burst (X-rays, gammas and neutrons). Depending on the type of weapon and its burst height, the prompt radiation can be deposited in the air anywhere from microseconds to even milliseconds. We assumed a time variation such that about 80 percent of the radiation is deposited in the air by  $10^{-5}$  seconds for the multiburst calculations. This is fairly typical of many weapons detonated close to the ground. In this set of runs eight bursts, thirty seconds apart and each having a total ionization of  $6 \times 10^{15}$  ion-pairs, were calculated. Both the new and old chemistry were used. In none of these calculations was the temperature allowed to rise. The single burst, for which the total ionization was  $6 \times 10^{16}$  ion-pairs, was also calculated with both the old and the new chemistry. The temperature was allowed to rise as the energy was deposited and for  $6 \times 10^{16}$  ion-pairs the temperature rise is about 350 K. In addition the bulk of the ionization (about 80 percent) was produced by about  $10^{-4}$  seconds rather than by  $10^{-5}$  seconds as in the multiburst calculations.

In the multiburst calculations, i.e., the set of eight consecutive bursts, the  $\text{HNO}_3$  production was, surprisingly, the same for the old chemistry and the new. After the first burst the  $\text{HNO}_3$  production was about 0.05 per ion-pair which quickly rose with subsequent bursts to about 0.10  $\text{HNO}_3$  molecule per ion-pair. Apparently the tying up of the  $\text{NO}_2$  in  $\text{HO}_2\text{NO}_2$  decreased the  $\text{HNO}_3$  production as much as the tying up of the  $\text{HO}_2$ .

In addition, during the time of major ion-ion recombination the negative ion distribution has not yet developed fully and  $\text{NO}_2^-$  is the major ion rather than  $\text{NO}_3^-$ . Thus recombination with  $\text{H}_3\text{O}^+(\text{H}_2\text{O})_n$  will yield  $\text{HNO}_2$  rather than  $\text{HNO}_3$ .

The  $\text{HNO}_2$  production is, therefore, larger than the  $\text{HNO}_3$  production. For the new chemistry runs it is about 0.16 per ion pair and for the runs with the old chemistry it is about 0.09.

The  $\text{HNO}_3$  production is much less than that for the calculation described in the last section, i.e., when the ionization dose is spread out over a couple of minutes, and the  $\text{HNO}_2$  production is greater. One of the reasons for this is  $\text{NO}_2^-$  is the major negative ion during the major deionization phase. Another reason is that the OH disappears shortly after the ionization pulse decays while  $\text{NO}_2$  takes time to appear. The overlap between the two is the only time  $\text{HNO}_3$  can form by  $\text{OH} + \text{NO}_2$  combination and this overlap time is short. On the other hand  $\text{NO}$  is formed almost immediately when the ionization pulse is turned on so that  $\text{NO} + \text{OH}$  combination is favored. Still another reason is that in the nuclear case the electron density is large enough to compete with the negative ions in neutralizing the positive ions. Thus reaction 26 contributes less to production of  $\text{HNO}_3$  than in the experiment.

We see that the timing of the ionization pulse is a critical factor in the production of  $\text{HNO}_3$ . For a given total ionization the longer it takes the energy to be deposited the more  $\text{HNO}_3$  will be produced. The single pulse calculations for a total ionization of  $6 \times 10^{16}$  ion-pairs and a  $10^{-4}$  second ionization pulse should give the same answers for  $\text{HNO}_3$  production as the multiburst calculations since the total ionization is about the same and the combined pulse time is also the same. The  $\text{HNO}_3$  production was, in fact, much smaller. The value was about 0.03  $\text{HNO}_3$  per ion-pair for the new chemistry and about 0.02 for the old. The  $\text{HNO}_2$  production was about 0.08 and 0.05, respectively. This is a factor of about

three, for the  $\text{HNO}_3$ , and a factor of two, for the  $\text{HNO}_2$ , less than the multiburst results. The difference is due to the fact that in the single burst calculations the gas temperature was allowed to rise as energy was deposited. This 300 or so degree rise in temperature effects the  $\text{HNO}_3$  production in at least two ways. The first way, already noted in a previous section, is to prevent a significant amount of  $\text{HO}_2\text{NO}_2$  from being formed. The second way is to reduce the value of the ion-ion recombination coefficient. This rate coefficient is assumed to have a  $T^{-2.5}$  dependence and doubling the temperature reduces the coefficient by about a factor of six. This means that electrons will compete more successfully with the negative ions for positive ions with which to recombine. This, in turn, means that reactions 19 and 20 will produce less  $\text{HNO}_2$  as well as  $\text{HNO}_3$ .

To sum up our results regarding  $\text{HNO}_3$ , the nuclear case will not produce nearly as much per ion-pair as was produced in the experiment. This is primarily due to the fact that in the nuclear case the bulk of the ionization is produced very quickly. If the temperature of the gas is raised significantly by the energy deposition the yield of  $\text{HNO}_3$  per ion pair will be reduced further.

The attachment rate due to attachment to  $\text{O}_2$  at sea level is between  $5 \times 10^7$  and  $10^8 \text{ sec}^{-1}$ . The attachment rate coefficient of  $\text{HNO}_3$  is  $5 \times 10^{-8} \text{ cm}^3/\text{sec}$  at 300 K. (The rate coefficient may decrease with increasing temperature but this is unknown.) Therefore concentrations of  $\text{HNO}_3$  of about  $10^{15} \text{ cm}^{-3}$  or more could change the total attachment significantly. With a value of 0.03  $\text{HNO}_3$  per ion-pair this would require a total ionization of about  $3 \times 10^{16}$  ion-pairs or more for the  $\text{HNO}_3$  attachment to dominate the attachment. Ionization doses of this magnitude are quite possible within a kilometer or so of a large yield burst.

The value of the  $\text{HNO}_3$  production could be significantly larger than the value of 0.03 obtained in the single burst calculation. Types of

weapons which radiate the bulk of their energy over millisecond or greater times would yield more  $\text{HNO}_3$ . The production of  $\text{HNO}_3$  could also be increased by the reasons given in the last section, i.e., if the amount of odd nitrogen produced initially per ion pair is larger than we have shown in Table 1, or if the rate coefficient for reaction 22 is smaller than we have used, or if an efficient mechanism exists which converts  $\text{HNO}_2$  to  $\text{HNO}_3$ . This last possibility could be quite important since in the nuclear cases we have calculated, the  $\text{HNO}_2$  production was two to three times the  $\text{HNO}_3$  production.

The amount of  $\text{N}_2\text{O}$  produced in all the nuclear cases we calculated was about 0.18 per ion-pair. For  $\text{N}_2\text{O}$  to compete as an efficient attacher of electrons the  $\text{N}_2\text{O}$  must be in excited vibrational states corresponding to the gas being heated to near 1000K or so. This requires an ionization dose of between  $10^{17}$  and  $2 \times 10^{17}$  ion-pairs. Under these conditions the  $\text{N}_2\text{O}$  can become a significant electron attacher.

The only other species produced in the single burst nuclear case in quantities large enough to be an appreciable attacher of electrons is  $\text{H}_2\text{O}_2$ . It is produced at the rate of about 0.05 per ion-pair. The reaction



is energetically very nearly resonant so if this reaction has a large rate coefficient the reverse reaction should also have a large coefficient. This is not the case.<sup>8</sup> However, as is the case with other molecules such as  $\text{N}_2\text{O}$ , the rate may increase dramatically when the  $\text{H}_2\text{O}_2$  is in an excited vibrational state. Thus when the deposition is large enough to heat the gas significantly,  $\text{H}_2\text{O}_2$  may become an important electron attacher.

## SECTION 8 BOMBLIGHT EFFECTS

For a certain time after burst the fireball will radiate a considerable amount of energy in the visible and ultraviolet regions of the spectrum. This energy can impact the chemistry through photoexcitation, photodissociation and photodetachment processes.

Although the temperature of the fireball during the radiative growth phase can be very high (many eV), the radiation does not escape the fireball. It is not until what is called "second maximum" in the radiative output that the bulk of the radiative energy escapes. For large yield bursts this occurs at a time of the order of a second and the radiating temperature is about 6000 K. Since this is the same radiating temperature as the sun we can obtain the photochemical rates at the point in question by taking those derived for sunlight at the top of the atmosphere and multiply by the ratio of the solid angle subtended by the fireball to the solid angle subtended by the sun. This yields for the photochemical rate,  $k$

$$k = 4.6 \times 10^4 \left(\frac{R}{d}\right)^2 k_s \text{ sec}^{-1} \quad (33)$$

where  $R$  is the radius of the fireball,  $d$  is the distance from the burst point, and  $k_s$  is the corresponding sunlight photochemical rate.  $k$  and  $k_s$  are in units of  $\text{sec}^{-1}$ . For a nominal large yield burst the radius at first maximum is about 0.6 km. For  $d = 1.2$  km we have

$$k = 1.2 \times 10^4 k_s \text{ sec}^{-1} \quad (34)$$

We wish to know whether the photodetachment rate caused by these processes can ever dominate the ionization rate produced by the delayed gamma radiation from the weapon. To do this we use the detachment rate coefficients obtained by equation 34 for the various negative ions present and the negative ion distribution and obtain a value for the overall detachment of about 250 times the negative ion concentration,  $M^-$ . Virtually all of the detachment comes from the species  $O_2^-$ ,  $O^-$ ,  $NO_2^-$  and  $NO_3^-$ . For steady-state conditions, the value of  $M^-$  is given by<sup>7</sup>

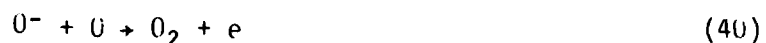
$$M^- = \sqrt{q/\alpha_i} \text{ cm}^{-3} \quad (35)$$

where  $q$  is the value of the ionizing source in  $\text{cm}^{-3}/\text{sec}$  and  $\alpha_i$  is the ion-ion recombination rate in  $\text{cm}^3/\text{sec}$ . The value of  $q$  at which the production of electrons by detachment is equal to the direct production by the ionizing source is given by

$$q = \frac{6.3 \times 10^4}{\alpha_i} \text{ cm}^{-3}/\text{sec} \quad (36)$$

For larger values of  $q$  the direct ionization will dominate the detachment. Using a value of  $1.4 \times 10^{-6} \text{ cm}^3/\text{sec}$  for  $\alpha_i$  we obtain a value from Equation 36 of about  $5 \times 10^{10} \text{ cm}^{-3}/\text{sec}$ . At about a second and a distance of 1.2 kilometers from the burst the ionization rate due to delayed gamma radiation is more than two orders of magnitude larger than  $5 \times 10^{10} \text{ cm}^{-3}/\text{sec}$ .<sup>9</sup> Thus, bomb-light photodetachment will not be an important factor in determining the electron density when compared to direct delayed gamma ionization. This has been confirmed by calculations using our chemistry code.

The bomb light can also indirectly affect the electron density via photodissociation. The primary candidates for these effects are  $O_3$  and  $NO_2$ . When an  $O_3$  photodissociates an atomic oxygen and an  $O_2(^1\Delta)$  are formed and both of these can chemically detach  $O_2^-$  and  $O^-$  via the reactions



The photodissociation of  $NO_2$  produces an atomic oxygen and an NO molecule. The NO can detach  $O^-$  by the reaction



More importantly the decrease in  $O_3$  and  $NO_2$  concentrations as a result of photodissociation causes an affect in the steady-state negative ion distribution. The transformation of initially produced  $O^-$  and  $O_2^-$  to more strongly bound negative ions, involves a number of intermediate negative ions such as  $O_3^-$  and  $CO_3^-$ .  $O_3$  is a vital reactant in the formation of these species.  $NO_2$  is involved in the further transformation of these negative ions to  $NO_2^-$  and  $NO_3^-$ , ions which are not as easily detached as  $O^-$  and  $O_2^-$ . A significant reduction of  $O_3$  and  $NO_2$ , particularly  $O_3$ , would slow down this evolution of  $O^-$  and  $O_2^-$  to  $NO_2^-$  and  $NO_3^-$  and would change the steady-state negative ion distribution to one in which the concentrations of  $O^-$  and  $O_2^-$  would be larger than before. This would, of course, increase both the photo and chemical detachment.

The sunlight photodissociation rates of  $O_3$  and  $NO_2$  are both about  $10^{-2} \text{ sec}^{-1}$ . Multiplying this by a factor given in Equation 34 yields

$$k = 120 \text{ sec}^{-1} \quad (42)$$

Adding this destruction mechanism to our code for  $O_3$  and  $NO_2$  did make an appreciable effect in the concentrations of these species, particularly for  $O_3$ . We also added the increased direct photodetachment by bomblight of all negative ions. The combined effects did increase the detachment significantly but still not enough to have detachment compete with the delayed gamma ionizing source. Thus the electron density was not affected significantly.

In addition, the effect of intervening  $O_3$  and  $NO_2$  in reducing the photon flux at the point in question was not included.  $O_3$ , in particular, has a rather large absorption cross-section and an average  $O_3$  density of only  $10^{13} \text{ cm}^{-3}$  or less between the fireball edge and the point in question would severely attenuate the dissociating light flux. Our calculations indicate enough  $O_3$  would be present to reduce the photon flux at least an order of magnitude or more.

If we were to move in closer to the fireball edge the effects of photodissociation of  $O_3$  and  $NO_2$  would increase. However, we would be encountering gas which would be significantly heated by the greater initial energy deposition and also by the outgoing shock wave. In this gas thermal dissociation would become important and would outweigh the photodissociation.

In summary, it does not seem that bomblight will have any first order effects on the electron densities in the air surrounding the burst.



## SECTION 9 CONCLUSIONS

Although the production of  $\text{HNO}_3$  in slowly irradiated air is large the yield is considerably less for the nuclear burst case where the irradiation time is typically quite short. Enough  $\text{HNO}_3$ , however, is produced in the nuclear case to make it potentially important as an attacker of electrons. In addition, there are a number of uncertainties in the formation processes leading to  $\text{HNO}_3$  production that might lead to an even higher production of  $\text{HNO}_3$ .

Significant quantities of  $\text{N}_2\text{O}$  are formed in the nuclear case but  $\text{N}_2\text{O}$  is only an important attacker of electrons in gas which has been heated to about 1000K or so. This might be accomplished by the initial energy deposition and the outgoing shock wave in a limited region near the burst.

Bomblight effects on the electron density are at most marginal. Bomblight effects might be important for low yield weapons for which the radiating temperature at second maximum is significantly larger than 6000 K. However, these effects would be limited to times much less than a second and to distances from the fireball edge of a fireball radius or less. For a low yield weapon this would be of the order of 50 meters or less.

## REFERENCES

1. Gilmore, F. R., Private communication, 1980 and Preliminary Revised Production Rate Distribution for Bombarded Air, Letter dated 28 May 1974, R & D Associates.
2. Meyers, B. F., and M. R. Schoonover, UV Photon and Electron Deposition in the Atmosphere, DNA 4068F, Science Applications Inc., August 1976 and Electron Energy Degradation in the Atmosphere, DNA 3513T, Science Applications Inc., January 1975.
3. Black, G., Private communication, 1980.
4. Hampson, R. F., Chemical Kinetics and Photochemical Data Sheets for Atmospheric Reactions, Department of Transportation, Report No. FAA-EE-80-17, April 1980.
5. Jones, A. R., Radiation-Induced Reactions in the  $N_2 - O_2 - H_2O$  System, Radiation Research, 10, 655 (1959).
6. Baulch, et. al., Evaluated Kinetic and Photochemical Data for Atmospheric Chemistry, J. Phys. Chem. Ref. Data, 11, 327 (1982).
7. DeMore, W. B., Chemical Kinetics and Photochemical Data for Use in Stratospheric Modeling: Evaluation Number 5, Jet Propulsion Laboratory Publication 82-57, 1982.
8. Albritton, D. L., Ion-Neutral Reaction-Rated Constants Measured in Flow Reactors Through 1977, Atomic Data and Nuclear Tables 22, 1 (1978).
9. Knapp, W. S. and K. Schwartz, Aids for the Study of Electromagnetic Blackout, DNA 3449H, General Electric TEMPO, February 1975.

## DISTRIBUTION LIST

### DEPARTMENT OF DEFENSE

Defense Advanced Rsch Proj Agency  
ATTN: GSD, R. Alewene  
ATTN: STO, W. Kurowski

Defense Communications Agency  
ATTN: Code 230  
ATTN: Code 205  
ATTN: J300 for Yen-Sun Fu

Defense Communications Engineer Center  
ATTN: Code R410, N. Jones  
ATTN: Code R123, Tech Lib

Defense Intelligence Agency  
ATTN: DB-4C  
ATTN: DB, A. Wise  
ATTN: DT-1B  
ATTN: Dir  
ATTN: DC-7B

Defense Nuclear Agency  
ATTN: STNA  
ATTN: RAEI  
ATTN: NAWI  
ATTN: RAAE, P. Lunn  
ATTN: NATF  
4 cy ATTN: STTI/CA  
3 cy ATTN: RAAE

Defense Technical Info Ctr  
12 cy ATTN: DD

Dep Under Secy of Defense, Comm, Cmd, Cont & Intell  
ATTN: Dir of Intelligence Sys

Field Command/DNA, Det 1  
Lawrence Livermore Lab  
ATTN: FC-1

Field Command, Defense Nuclear Agency  
ATTN: FCPR  
ATTN: FCTXE  
ATTN: FCTT, W. Summa

Interservice Nuclear Weapons School  
ATTN: TTV

Joint Chiefs of Staff  
ATTN: C3S  
ATTN: C3S Eval Office, HD00

Joint Data System Support Ctr  
ATTN: G510, G. Jones  
ATTN: C-312, R. Mason  
ATTN: G510, P. Bird

Joint Strat Tgt Planning Staff  
ATTN: JPPFD  
ATTN: JPSS  
ATTN: JPTM  
ATTN: JLKS  
ATTN: JLK, DNA Rep

National Security Agency  
ATTN: B-43, C. Goedeke  
ATTN: W-36, O. Bartlett

### DEPARTMENT OF DEFENSE (Continued)

Under Secy of Def for Rsch & Engrg  
ATTN: Strat & Space Sys, OS  
ATTN: Strat & Theater Nuc For, B. Stephan

WWMCCS System Engineering Org  
ATTN: R. Crawford

### DEPARTMENT OF THE ARMY

Army Logistics Management Ctr  
ATTN: DLSIE

Assistant Chief of Staff for Automation & Comm  
ATTN: DAMO-C4, P. Kenny

Atmospheric Sciences Laboratory  
ATTN: DELAS-E0, F. Niles

BMD Advanced Technology Ctr  
ATTN: ATC-R, W. Dickinson  
ATTN: ATC-T, M. Capps

BMD Systems Command  
ATTN: BMDS-C-LEE, R. Webb  
2 cy ATTN: BMDS-C-HW

Dep Ch of Staff for Ops & Plans  
ATTN: DAMO-RQC, C2 Div

Harry Diamond Laboratories  
ATTN: DELHD-NW-P, 20240  
ATTN: DELHD-NW-R, R. Williams, 22000

US Army Chemical School  
ATTN: ATZN-CM-CS

US Army Comm-Elec Engrg Instal Agency  
ATTN: CC-CE-TP, W. Nair

US Army Communications Command  
ATTN: CC-OPS-WR, H. Wilson  
ATTN: CC-OPS-W

US Army Communications R&D Command  
ATTN: DRDCO-COM-RY, W. Kesselman

US Army Foreign Science & Tech Ctr  
ATTN: DRXST-SD

US Army Material Command  
ATTN: DRCLDC, J. Bender

US Army Nuclear & Chemical Agency  
ATTN: Library

US Army Satellite Comm Agency  
ATTN: Doc Control

US Army TRADOC Sys Analysis Actv  
ATTN: ATAA-TCC, F. Payan, Jr  
ATTN: ATAA-PL  
ATTN: ATAA-TDC

DEPARTMENT OF THE NAVY

Joint Cruise Missiles Project Ofc  
ATTN: JCMG-707

Naval Air Systems Command  
ATTN: PMA 271

Naval Electronic Systems Command  
ATTN: Code 501A  
ATTN: Code 3101, T. Hughes  
ATTN: PME 117-20  
ATTN: PME 106-4, S. Kearney  
ATTN: PME 117-211, B. Kruger  
ATTN: PME 117-2013, G. Burnhard  
ATTN: PME 106, F. Diederich

Naval Intelligence Support Ctr  
ATTN: NISC-50

Naval Research Lab  
ATTN: Code 4720, J. Davis  
ATTN: Code 7500, B. Wald  
ATTN: Code 4780  
ATTN: Code 4700  
ATTN: Code 4187  
ATTN: Code 7950, J. Goodman  
ATTN: Code 6700  
ATTN: Code 4108, E. Szuszewicz

Naval Space Surveillance System  
ATTN: J. Burton

Naval Surface Weapons Center  
ATTN: Code F31

Naval Telecommunications Command  
ATTN: Code 341

Ofc of the Deputy Chief of Naval Ops  
ATTN: NOP 981N  
ATTN: NOP 941D  
ATTN: NOP 654, Strat Eval & Anal Br

Office of Naval Research  
ATTN: Code 412, W. Condell

Strategic Systems Project Office  
ATTN: NSP-43, Tech Lib  
ATTN: NSP-2141  
ATTN: NSP-2722

Theater Nuc Warfare Prj Office  
ATTN: PM-23, D. Smith

DEPARTMENT OF THE AIR FORCE

Air Force Geophysics Laboratory  
ATTN: OPR-1  
ATTN: LYD, K. Champion  
ATTN: CA, A. Stair  
ATTN: LIS, J. Buchau  
ATTN: R. Babcock  
ATTN: R. O'Neil

Air Force Satellite Ctrl Facility  
ATTN: WE

Air Force Weapons Laboratory  
ATTN: SUL  
ATTN: NTN

DEPARTMENT OF THE AIR FORCE (Continued)

Air Force Space Technology Ctr  
ATTN: YH

Air Force Flight Aeronautical Lab/AAAD  
ATTN: W. Hunt  
ATTN: A. Johnson

Air Logistics Command  
ATTN: OO-ALC/MM

Air University Library  
ATTN: AUL-LSE

Asst Chief of Staff, Studies & Analysis  
ATTN: AF/SASC, C. Rightmeyer

Ballistic Missile Office/DAA  
ATTN: ENSN  
ATTN: SYC, D. Kwan  
ATTN: ENSN, W. Wilson

Deputy Chief of Staff, Research, Dev, & Acq  
ATTN: AFRDQI  
ATTN: AFRDS, Space Sys & C3 Dir  
ATTN: AFXOKCD  
ATTN: AFXOKS  
ATTN: AFXOKT

Electronic Systems Div  
ATTN: SCS-2, G. Vinkels  
ATTN: SCS-1E

Foreign Technology Div  
ATTN: NUIS, Library  
ATTN: TQTD, B. Ballard

Rome Air Development Center  
ATTN: EEP, J. Rasmussen  
ATTN: EEPS, P. Kossey

Rome Air Development Center  
ATTN: TSLD  
ATTN: OCSA, R. Schneible  
ATTN: OCS, V. Coyne

Space Command  
ATTN: DC, T. Long

Strategic Air Command  
ATTN: DCX  
ATTN: DCZ  
ATTN: NRI/STINFO Library  
ATTN: XPFC  
ATTN: XPFS  
ATTN: XPQ

DEPARTMENT OF ENERGY

Department of Energy, GTN  
ATTN: DP-233

OTHER GOVERNMENT AGENCIES

US Department of State  
ATTN: PM/STM

Central Intelligence Agency  
ATTN: OSWR/SSD for K. Feuerpfetl

OTHER GOVERNMENT AGENCIES (Continued)

National Oceanic & Atmospheric Admin  
ATTN: R. Grubb  
ATTN: F. Fehsenfeld

National Bureau of Standards  
ATTN: Sec Officer for R. Moore

Institute for Telecommunications Sciences  
ATTN: A. Jean  
ATTN: L. Berry  
ATTN: W. Utlaut

DEPARTMENT OF ENERGY CONTRACTORS

EG&G, Inc  
ATTN: J. Colvin  
ATTN: D. Wright

Univ of CA, Lawrence Livermore National Lab  
ATTN: Tech Info Dept Lib

Los Alamos National Lab  
ATTN: D. Sappenfield  
ATTN: G-6, E. Jones

Sandia National Laboratories  
ATTN: D. Dahlgren  
ATTN: Space Project Div  
ATTN: Tech Lib 3141  
ATTN: D. Thornbrough  
ATTN: Org 1250, W. Brown  
ATTN: Org 1231, R. Backstrom

Sandia National Laboratories  
ATTN: T. Cook  
ATTN: B. Murphey  
ATTN: R. Grossman

DEPARTMENT OF DEFENSE CONTRACTORS

Aerospace Corp  
ATTN: S. Mewaters

Aerospace Corp  
ATTN: J. Kluck  
ATTN: I. Garfunke  
ATTN: D. Olsen  
ATTN: J. Straus  
ATTN: R. Slaughter  
ATTN: T. Salmi  
ATTN: V. Josephson  
ATTN: K. Cho  
ATTN: D. Whelan

Analytical Systems Engineering Corp  
ATTN: Security

Analytical Systems Engineering Corp  
ATTN: Radio Sciences

Austin Research Assoc  
ATTN: J. Thompson  
ATTN: B. Moore  
ATTN: M. Sloan  
ATTN: J. Uglum

BDM Corp  
ATTN: L. Jacobs  
ATTN: T. Neighbors

DEPARTMENT OF DEFENSE CONTRACTORS (Continued)

Berkeley Rsch Associates, Inc  
ATTN: J. Workman  
ATTN: S. Brecht

Boeing Co  
ATTN: MS 8K-85, Dr S. Tashird

Boeing Co  
ATTN: G. Hall

BR Communications  
ATTN: J. McLaughlin

University of California at San Diego  
ATTN: H. Booker

California Research & Tech, Inc  
ATTN: M. Rosenblatt

Charles Stark Draper Lab, Inc  
ATTN: D. Cox  
ATTN: J. Gilmore  
ATTN: A. Tetewski

Communications Satellite Corp  
ATTN: G. Hyde  
ATTN: D. Fang

Computer Sciences Corp  
ATTN: F. Eisenbarth

Cornell University  
ATTN: D. Farley, Jr  
ATTN: M. Kelly

Electrospace Systems, Inc  
ATTN: H. Logston

EOS Technologies, Inc  
ATTN: B. Gabbard  
ATTN: W. Lelevier

General Electric Co  
ATTN: R. Juner  
ATTN: A. Steinmayer  
ATTN: C. Zierdt

General Electric Co  
ATTN: G. Millman

General Research Corp  
ATTN: B. Bennett

GTE Communications Products Corp  
ATTN: H. Gelman

GTE Government Systems Corp  
ATTN: R. Steinhoff

Honeywell, Inc  
ATTN: A. Kearns, MS924-3  
ATTN: G. Terry, Avionics Dept

Horizons Technology, Inc  
ATTN: R. Kruger

HSS, Inc  
ATTN: D. Hansen

DEPARTMENT OF DEFENSE CONTRACTORS (Continued)

IBM Corp  
ATTN: H. Ulander

Institute for Defense Analyses  
ATTN: E. Bauer  
ATTN: H. Wolfhard  
ATTN: J. Aein

ITT Corp  
ATTN: G. Wetmore

ITT Corp  
ATTN: Technical Library

JAYCOR  
ATTN: H. Dickinson

JAYCOR  
ATTN: J. Sperling

Johns Hopkins University  
ATTN: K. Potocki  
ATTN: T. Evans  
ATTN: J. Newland  
ATTN: R. Stokes  
ATTN: J. Phillips  
ATTN: C. Meng

Kaman Sciences Corp  
ATTN: E. Conrad

Kaman Tempo  
ATTN: DASAC

Kaman Tempo  
ATTN: DASAC  
ATTN: B. Gambill

Litton Systems, Inc  
ATTN: B. Zimmer

Lockheed Missiles & Space Co, Inc  
ATTN: Dept 60-12  
2 cy ATTN: D. Churchill, Dept 62-A1

Lockheed Missiles & Space Co, Inc  
ATTN: J. Kumer  
ATTN: R. Sears

MIT Lincoln Lab  
ATTN: D. Towle  
ATTN: V. Vitto  
ATTN: N. Doherty

M/A Com Linkabit Inc  
ATTN: I. Jacobs  
ATTN: H. Van Trees  
ATTN: A. Viterbi

Magnavox Govt & Indus Electronics Co  
ATTN: G. White

Maxim Technologies, Inc  
ATTN: J. Marshall  
ATTN: E. Tsui  
ATTN: R. Morganstern

McDonnell Douglas Corp  
ATTN: W. Olson

DEPARTMENT OF DEFENSE CONTRACTORS (Continued)

Meteor Communications Corp  
ATTN: R. Leader

Mission Research Corp  
ATTN: G. McCartor  
ATTN: F. Gugliano  
ATTN: Tech Library  
ATTN: F. Fajen  
ATTN: R. Bogusch  
ATTN: R. Hendrick  
ATTN: D. Knepp  
ATTN: S. Gutsche  
ATTN: R. Dana  
ATTN: C. Lauer  
ATTN: R. Bigoni  
2 cy ATTN: M. Scheibe  
5 cy ATTN: Doc Control

Mitre Corp  
ATTN: A. Kymmel  
ATTN: G. Harding  
ATTN: C. Callahan

Mitre Corp  
ATTN: W. Hall  
ATTN: W. Foster  
ATTN: M. Horrocks

Pacific-Sierra Research Corp  
ATTN: E. Field, Jr  
ATTN: F. Thomas  
ATTN: H. Brode, Chairman SAGE

Pennsylvania State University  
ATTN: Ionospheric Research Lab

Photometrics, Inc  
ATTN: I. Kofsky

Physical Dynamics, Inc  
ATTN: E. Fremouw  
ATTN: J. Secan

Physical Research, Inc  
ATTN: J. Devore  
ATTN: J. Thompson

Physical Research, Inc  
ATTN: R. Deliberis  
ATTN: T. Stephens  
ATTN: K. Schueter

R&D Associates  
ATTN: M. Gantsweg  
ATTN: C. Greifinger  
ATTN: F. Gilmore  
ATTN: H. Ory  
ATTN: R. Turco  
ATTN: W. Wright  
ATTN: W. Karzas  
ATTN: G. Stcyr  
ATTN: P. Haas

R&D Associates  
ATTN: B. Yoon

Rand Corp  
ATTN: B. Bennett

DEPARTMENT OF DEFENSE CONTRACTORS (Continued)

Rand Corp

ATTN: C. Crain  
ATTN: E. Bedrozian  
ATTN: P. Davis

Riverside Research Institute  
ATTN: V. Trapani

Rockwell International Corp  
ATTN: S. Quilici

Rockwell International Corp  
ATTN: R. Buckner

Science Applications, Inc  
ATTN: M. Cross

SRI International

ATTN: C. Rino  
ATTN: J. Petrickes  
ATTN: D. Neilson  
ATTN: R. Livingston  
ATTN: M. Baron  
ATTN: R. Leadabrand  
ATTN: W. Chesnut  
ATTN: W. Jaye  
ATTN: G. Smith  
ATTN: A. Burns  
ATTN: G. Price  
ATTN: R. Tsunoda

Stewart Radiance Lab  
ATTN: R. Huppi

DEPARTMENT OF DEFENSE CONTRACTORS (Continued)

Science Applications, Inc

ATTN: C. Smith  
ATTN: D. Sachs  
ATTN: D. Hamlin  
ATTN: E. Straker  
ATTN: L. Linson

Swerling, Manasse & Smith, Inc  
ATTN: R. Manasse

Toyon Research Corp  
ATTN: J. Garbarino  
ATTN: J. Ise

TRW Electronics & Defense Sector  
ATTN: R. Plebuch

Utah State University

Attention Sec Control Ofc for  
ATTN: A. Steed  
ATTN: D. Burt  
ATTN: K. Baker, Dir Atmos & Space Sci  
ATTN: L. Jensen, Elec Eng Dept

Visidyne, Inc

ATTN: H. Smith  
ATTN: J. Carpenter  
ATTN: W. Reidy  
ATTN: O. Shepard





**END**

**FILMED**

**6-85**

**DTIC**